

Single Sparse Graph Enhanced Expectation Propagation Algorithm Design for Uplink MIMO-SCMA

Qu Luo*, Jing Zhu*, Gaojie Chen*, Pei Xiao* and Rahim Tafazolli*

* University of Surrey, Guildford, GU2 7XH, Surrey, U. K.

Email: {q.u.luo, j.zhu, gaojie.chen, p.xiao, r.tafazolli}@surrey.ac.uk.

Abstract—Sparse code multiple access (SCMA) and multiple input multiple output (MIMO) are considered as two efficient techniques to provide both massive connectivity and high spectrum efficiency for future machine-type wireless networks. This paper proposes a single sparse graph (SSG) enhanced expectation propagation algorithm (EPA) receiver, referred to as SSG-EPA, for uplink MIMO-SCMA systems. Firstly, we reformulate the sparse codebook mapping process using a linear encoding model, which transforms the variable nodes (VNs) of SCMA from symbol-level to bit-level VNs. Such transformation facilitates the integration of the VNs of SCMA and low-density parity-check (LDPC), thereby emerging the SCMA and LDPC graphs into a SSG. Subsequently, to further reduce the detection complexity, the message propagation between SCMA VNs and function nodes (FNs) are designed based on EPA principles. Different from the existing iterative detection and decoding (IDD) structure, the proposed EPA-SSG allows a simultaneously detection and decoding at each iteration, and eliminates the use of interleavers, de-interleavers, symbol-to-bit, and bit-to-symbol LLR transformations. Simulation results show that the proposed SSG-EPA achieves better error rate performance compared to the state-of-the-art schemes.

Index Terms—Multiple input multiple output (MIMO), Sparse code multiple access (SCMA), factor graph, expectation propagation algorithm (EPA), iterative detection and decoding (IDD), single sparse graph (SSG).

I. INTRODUCTION

Non-orthogonal multiple access (NOMA) has been envisioned as a promising multiple access technique to support diverse traffic with stringent requirements, such as high spectral efficiency, massive connectivity and high-level quality of service (QoS), for the beyond fifth generation (B5G) and sixth-generation (6G) networks [1]. By enabling overloaded transmission of multiple users, existing NOMA techniques can be primarily categorized into power-domain NOMA [2], [3] and code-domain NOMA (CD-NOMA) [4]. Sparse code multiple access (SCMA) is a representative CD-NOMA scheme which can achieve maximum-likelihood decoding performance with low complexity [5]. Furthermore, multiple-input multiple-output (MIMO) has been acknowledged as an enabling technique for enhancing spectral efficiency by leveraging spatial multiplexing or diversity. Consequently, the integration of SCMA with MIMO, known as MIMO-SCMA, has gained increasing attention due to its enhanced spectral efficiency and error rate performance [6]–[8].

By utilizing the sparsity structure in SCMA, message passing algorithm (MPA) has been employed to achieve near-optimal error rate performance with lower complexity compared to maximum likelihood detection [9]. However, the complexity of MPA increases exponentially with the codebook size M and the colliding users at each resource node. Therefore, many low-complexity detection approaches have also been proposed for SCMA [7], [8]. A notable example is the expectation propagation algorithm (EPA) for low-complexity detection in MIMO-SCMA. The use of EPA for uplink MIMO-SCMA detection was initially introduced in [7]. Later on, in [8], an EPA structure was developed for MIMO-SCMA with multi-antenna users based on the extended factor graph, where the computational complexity was further reduced by introducing QR decomposition and resource edge cluster-based decentralized factor node processing. In addition, an approximate EPA was proposed in [10], where the message passing at the variable and function nodes, and the log likelihood ratio calculation were simplified to reduce the detection complexity. The authors [11] proposed a decentralized processing scheme for low-complexity detection in uplink massive MIMO-SCMA systems by utilizing the EPA framework. The main idea is to partition the base station antennas into multiple independent antenna clusters.

Despite a rich body of works on low-complexity detection design, there is a limited focus on the joint optimization of detection and decoding design for MIMO-SCMA systems. The turbo like iterative detection and decoding (IDD), referred to as turbo-IDD, has been widely investigated for coded SCMA systems [12], [13]. Notable examples include [12] and [13]. In the turbo-IDD scheme, the SCMA detector and channel decoder are iteratively executed with a certain number of inner iterations independently for each outer iteration. However, the performance of the turbo-IDD is generally limited as the inefficient message passing between SCMA detector and channel decoder. Benefiting from the sparse structures of the SCMA factor graph and Tanner graph of LDPC, the joint detection and decoding (JDD) has been proposed for enhancing error rate performance by fully leveraging system diversity and coding gains [14], [15]. The JDD structure treats SCMA detector and turbo decoder as a joint factor graph, thereby improving the error rate performance and facilitating convergence. For exam-

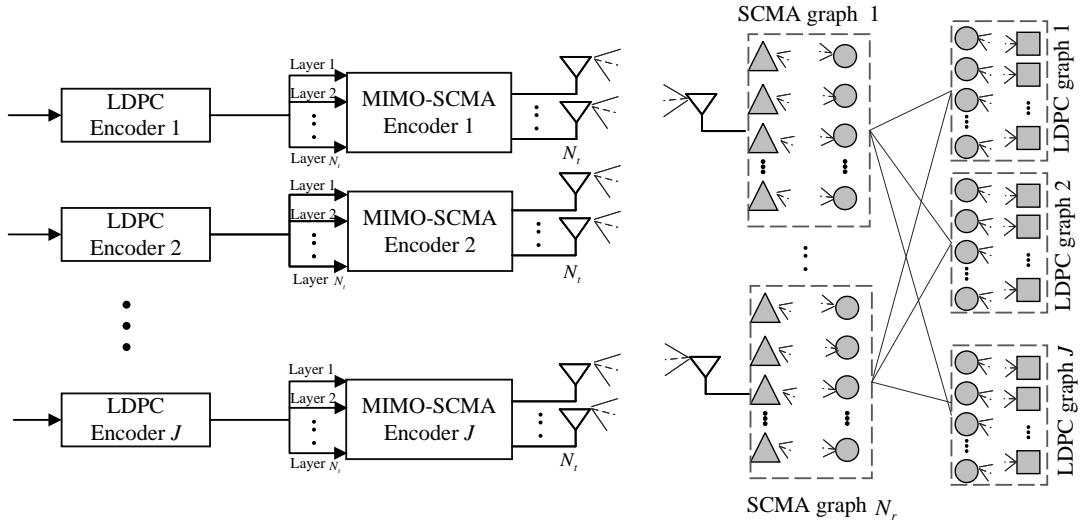


Fig. 1: System model of uplink MIMO-SCMA.

ple, the authors in [15] proposed an EPA-aided JDD structure for uplink MIMO-SCMA, which showed that the proposed JDD-EPA receiver achieves significantly lower complexity and faster convergence rate than the turbo-IDD receiver. It is noted that the messages between the SCMA detector and channel decoder in the JDD-EPA receiver still propagate sequentially.

In this paper, we propose a single sparse graph (SSG) enhanced EPA receiver, referred to as SSG-EPA, for uplink MIMO-SCMA systems. Unlike the JDD receiver, the detection and decoding in the proposed SSG-EPA receiver are performed simultaneously and in a joint manner at each iteration, eliminating the use of interleavers, de-interleavers, symbol-to-bit, and bit-to-symbol LLR transformations. By reformulating the codebook with a linear encoding model, the variable nodes (VNs) of SCMA can be transformed from symbol-level VNs to bit-level VNs. Consequently, the VNs of low-density parity-check (LDPC) codes and SCMA can be merged, leading to the proposed SSG. In addition, the EPA has been proposed for low complexity detection and the message propagation in the proposed EPS-SSG has been discussed in detail. Simulation results show that the proposed SSG-EPA is able to achieve low-detection complexity, fast convergence rate, and good bit error rate performance¹.

II. SYSTEM MODEL

We consider an uplink MIMO-SCMA system with J users multiplexed over K resource nodes (RNs), e.g., the OFDM subcarriers. The SCMA overloading is defined as $\lambda = J/K$, which is larger than 100%. The base station (BS) is equipped with N_r receive antennas and each user is equipped with N_t transmit antennas, hereafter, we use $N_t \times N_r$ to denote

¹Notations: Bold uppercase, bold lowercase and lowercase letters denote matrices, vectors and scalars, respectively. $\mathbb{C}^{k \times n}$ and $\mathbb{B}^{k \times n}$ denote the $(k \times n)$ -dimensional complex and binary matrix spaces, respectively. $\text{diag}(\mathbf{x})$ gives a diagonal matrix with the diagonal vector of \mathbf{x} . $(\cdot)^T$ and $(\cdot)^H$ denote the transpose and the Hermitian transpose operation, respectively. $\mathcal{CN}(0, 1)$ denotes the complex distribution with zero mean and unit variance.

the MIMO configuration. Fig. 1 shows system model of an uplink SCMA. During transmission, the input message data are first encoded with a channel code. Then, the encoded bits are divided into N_t layers for multiplexing. The SCMA encoder of user j maps the encoded bits to an SCMA codeword $\mathbf{x}_j^{(n_t)} \in \mathbb{C}^{K \times 1}$ selected from the layer-specific complex codebook on the n_t th transmit antenna, which is denoted as $\mathcal{X}_j^{n_t} \in \mathbb{C}^{K \times M}$. In this paper, we assume the codebook for each antenna is the same, thus the superscript is omitted. The detailed mapping process will be discussed later. In a standard SCMA with single-input single-output, each codeword has only N nonzero entries and the positions of the non-zeros elements remain the same within a codebook. Such a sparse structure can efficiently be represented by an indicator graph matrix, denoted by \mathbf{F} , which illustrates the sharing of the RNs among multiple VNs. An element of \mathbf{F} is defined as $f_{k,j}$ which takes the value of 1 if and only if VN v_j is connected to RN r_k and 0 otherwise. In this paper, the following basic indicator matrix with $K = 4, J = 6$ and $N = 2$ is considered [16]:

$$\mathbf{F}_{4 \times 6} = \begin{bmatrix} 0 & 1 & 1 & 0 & 1 & 0 \\ 1 & 0 & 1 & 0 & 0 & 1 \\ 0 & 1 & 0 & 1 & 0 & 1 \\ 1 & 0 & 0 & 1 & 1 & 0 \end{bmatrix}. \quad (1)$$

The received vector at the n_r th antenna of the BS is given by

$$\mathbf{y}^{n_r} = \sum_{j=1}^J \sum_{n_t=1}^{N_t} \text{diag}(\mathbf{h}_j^{(n_r, n_t)}) \mathbf{x}_j^{n_t} + \mathbf{z}^{n_r}, \quad (2)$$

where $n_r = 1, 2, \dots, N_r$, and $\mathbf{h}_j^{(n_r, n_t)} \in \mathbb{C}^{K \times 1}$ is the channel vector from the n_t th transmit antenna to the n_r th receive antenna of user j , $\mathbf{z}^{n_r} \in \mathbb{C}^{K \times 1}$ denotes the independent additive white Gaussian noise (AWGN) vector at the n_r th antenna of the BS, $\mathbf{y}^{n_r} = [y_1^{n_r}, y_2^{n_r}, \dots, y_K^{n_r}]^T$ denotes the received signal vector on the BS. Let $\mathbf{y} \equiv [\mathbf{y}^{1,T}, \mathbf{y}^{2,T}, \dots, \mathbf{y}^{N_r,T}]^T \in$

$\mathbb{C}^{N_r J \times 1}$ collect the received signal from N_r antennas, then the received signal can be re-written as

$$\mathbf{y} = \sum_{j=1}^J \mathbf{H}_j \mathbf{x}_j + \mathbf{z}, \quad (3)$$

where $\mathbf{x}_j \equiv [\mathbf{x}_j^{1,T}, \mathbf{x}_j^{2,T}, \dots, \mathbf{x}_j^{N_t,T}]^T \in \mathbb{C}^{N_t J \times 1}$ denotes the transmitted signal vector, $\mathbf{z} \equiv [\mathbf{z}^1,T, \mathbf{z}^2,T, \dots, \mathbf{z}^{N_t,T}]^T \in \mathbb{C}^{N_t J \times 1}$ denotes the complex AWGN noise vector, and $\mathbf{H}_j \in \mathbb{C}^{N_r K \times N_t K}$ denotes the MIMO channel matrix from the j th UE to the BS, which takes the following expression

$$\mathbf{H}_j \equiv \begin{bmatrix} \text{diag}(\mathbf{h}_j^{(1,1)}) & \text{diag}(\mathbf{h}_j^{(1,2)}) & \dots & \text{diag}(\mathbf{h}_j^{(1,N_t)}) \\ \text{diag}(\mathbf{h}_j^{(2,1)}) & \text{diag}(\mathbf{h}_j^{(2,2)}) & \dots & \text{diag}(\mathbf{h}_j^{(2,N_t)}) \\ \vdots & \vdots & \ddots & \vdots \\ \text{diag}(\mathbf{h}_j^{(N_r,1)}) & \text{diag}(\mathbf{h}_j^{(N_r,2)}) & \dots & \text{diag}(\mathbf{h}_j^{(N_r,N_t)}) \end{bmatrix}. \quad (4)$$

III. THE PROPOSED SINGLE GRAPH DESIGN

A. Preliminary

This section introduces the preliminaries in MIMO-SCMA detection and decoding.

1) *Turbo receiver with iterative detection and decoding (Turbo-IDD)*: In the Turbo-IDD structure, iterative messages are exchanged between the multiuser detector (MUD) and channel decoder. Denote $N_{\text{iter}}^{\text{MUD}}$ and $N_{\text{iter}}^{\text{DEC}}$ by the number of inner iterations of the MUD and channel decoder, respectively. Similarly, we further denote $N_{\text{iter}}^{\text{out}}$ as the number of outer iterations.

2) *Joint detection and decoding*: In an LDPC coded SCMA system, both MUD and channel decoder can be represented with sparse factor graphs. By merging the SCMA factor and LDPC graph into a integrated one, the belief message are able to exchange efficiently over an aggregated factor graph associated to both the sparse codebooks and LDPC codes.

Although the JDD shows significant performance improvement over the Turbo-IDD receiver, the LLR exchange between the SCMA factor graph and LDPC graph makes belief message propagation inefficient. Specifically, the SCMA VNs need to transform the LLR of each codeword to bit-level LLRs and pass them to the deinterleaver. Similarly, the output bit-level LLRs from the LDPC VNs need to be transformed back to symbol LLRs. These LLR transformations and interleavers/deinterleavers prevent belief messages from propagating in a single graph manner. In this section, we present the proposed SSG design for MIMO-SCMA systems.

B. Codebook Reformulation

For conventional SCMA codebook, the encoder maps the input binary message to a codeword selected from a pre-defined codebook codebook, i.e.,

$$f_j: \mathbb{B}^{\log_2 M \times 1} \mapsto \mathcal{X}_j, \quad \text{i.e., } \mathbf{x}_j = f_j(\mathbf{b}_j), \quad (5)$$

where $\mathbf{b}_j = [b_{j,1}, b_{j,2}, \dots, b_{j,\log_2 M}]^T \in \{1, -1\}^{\log_2 M}$ stands for j th user's instantaneous input binary message vector,

$\mathcal{X}_j \in \mathbb{C}^{K \times M}$ denotes the codebook of j th user and f_j denotes the SCMA encoding process. It should be noted that the codebook is deigned with symmetric. In fact, many of existing SCMA codebooks has such property, which empowers the SCMA encoding process can be written as a linear encoding process. Namely,

$$\mathbf{x}_j = \mathbf{G}_j \mathbf{b}_j, \quad (6)$$

where $\mathbf{G}_j \in \mathbb{C}^{K \times \log_2 M}$ is the codebook generator matrix of the j th user. By collecting all the \mathbf{b}_j according to their corresponding integer values in ascending order, we form a $\log_2(M) \times M$ binary matrix \mathbf{B} . For example, when $M = 4$ and 16, we have

$$\mathbf{B} = \begin{bmatrix} - & + & - & + \\ - & - & + & + \end{bmatrix}, \quad (7)$$

and

$$\mathbf{B} = \begin{bmatrix} - & + & - & + & - & + & - & + & - & + & - & + & - & + & - & + \\ - & - & + & - & - & + & - & - & + & - & - & + & - & - & + & - \\ - & - & - & + & + & + & - & - & - & + & + & + & - & - & - & + \\ - & - & - & - & - & - & - & + & + & + & + & + & + & + & + & + \end{bmatrix}, \quad (8)$$

respectively, where “+” and “-” denote +1 and -1, respectively. It should be noted that the m th column of (7) and (8) are symmetric with their negative values of $(M - m)$ th column. Namely, the values at $(M - m)$ th column are equal to the negative of the value of m th column. Hence, for the codebook that also has such symmetric property, the codebook generator \mathbf{G}_j can be generated as [17]

$$\mathbf{G}_j = \mathcal{X}_j \mathbf{B}^T (\mathbf{B} \mathbf{B}^H)^{-1}. \quad (9)$$

Hence, the signal model of (2) can be rewritten as

$$\begin{aligned} \mathbf{y}^{(n_r)} &= \sum_{j=1}^J \sum_{n_t=1}^{N_t} \text{diag}(\mathbf{h}_j^{(n_r, n_t)}) \mathbf{G}_j \mathbf{b}_j^{(n_t)} + \mathbf{z}^{(n_r)} \\ &= \sum_{j=1}^J \sum_{n_t=1}^{N_t} \bar{\mathbf{H}}_j^{(n_r, n_t)} \mathbf{b}_j^{(n_t)} + \mathbf{z}^{(n_r)}, \end{aligned} \quad (10)$$

where $\bar{\mathbf{H}}_j^{(n_r, n_t)} = \text{diag}(\mathbf{h}_j^{(n_r, n_t)}) \mathbf{G}_j$ denotes the effective channel matrix.

C. The Proposed SSG-EPA

For the MIMO-SCMA system depicted in Fig. 1, the joint distribution $p(\mathbf{b}, \mathbf{y})$ can be respectively factorized as

$$\begin{aligned} p(\mathbf{y}, \mathbf{b}) &= p(\mathbf{y}|\mathbf{b})p(\mathbf{b}) \\ &= \prod_{n_t=1}^{N_t} \prod_{j=1}^J \prod_{m=1}^{\log_2 M} p(b_{j,m}^{n_t}) \prod_{n_r=1}^{N_r} \prod_{k=1}^K p(y_k^{n_r} | b_{j,m}^{n_t}). \end{aligned} \quad (11)$$

The SCMA factor graph can be designed to contain $JN_t \log_2 M$ VNs and $N_r K$ likelihood FNs. For easy of presentation, the SCMA VNs are denoted by $v_n^m, n = 1, 2, \dots, JN_t, m = 1, 2, \dots, \log_2 M$ and the FN at the k th subcarrier of n_r th receiver antenna is denoted as $f_k^{n_r}$. The corresponding factor graph representation of the proposed SSG is shown in Fig. 2. Note that the SCMA and LDPC VNs are all propagate messages in bit-levels, hence, it is reasonable to

place SCMA FNs (triangles) and LDPC CNs (rectangles) on one side, while drawing bit VNs (circles) on the other side. The LLR calculation of bit to symbol and symbol to bit are no longer required and the interleaver (deinterleaver) can also be eliminated as it can be emerged within the SSG.

In this paper, we consider the EPA as the MUD for low complexity detection. EPA is a Bayesian inference method designed to approximate the complex posterior belief distribution using a tractable distribution, typically a Gaussian distribution achieved through moment matching. Define the projection of a distribution p into a distribution set Φ as [8]

$$\text{Proj}_{\Phi}(p) = \arg \min_{q \in \Phi} \text{KL}(p||q), \quad (12)$$

where $\text{KL}(p||q)$ denotes the Kullback Leibler (KL) divergence that measures the similarity between the *a posteriori* belief distribution and the tractable distribution after projection. Namely, we have

$$\text{KL}(p||q) = \sum_{\mathbf{b}} p(\mathbf{b}|\mathbf{y}) \log \frac{p(\mathbf{b}|\mathbf{y})}{q(\mathbf{b}|\mathbf{y})}. \quad (13)$$

where \mathbf{b} denotes the transmitted message bits of J users. Denote $I_{v_n^m \rightarrow f_k^{n_r}}^t(b_n^m)$ and $I_{f_k^{n_r} \rightarrow v_n^m}^t(b_n^m)$ as the belief message propagated from VN v_n^m to FN $f_k^{n_r}$ and FN $f_k^{n_r}$ to VN v_n^m at the t th iteration, respectively. We further denote the set of SCMA VNs indices sharing the $f_k^{n_r}$ as $F(k, n_r)$, whereas the set of FN indices sharing the v_n^m is denoted by $V(n)$. According to the EP principles, the message update rule can be expressed as [15]:

$$I_{v_n^m \rightarrow f_k^{n_r}}^t(b_n^m) \propto \frac{\text{Proj}_{\Phi}(q_0^t(b_n^m))}{I_{f_k^{n_r} \rightarrow v_n^m}^{t-1}(b_n^m)}, \quad (14)$$

$$I_{f_k^{n_r} \rightarrow v_n^m}^t(b_n^m) \propto \frac{\text{Proj}_{\Phi}(q_{k, n_r}^t(b_n^m))}{I_{v_n^m \rightarrow f_k^{n_r}}^t(b_n^m)}, \quad (15)$$

where

$$q_0^l(b_n^m) \propto p_0(b_n^m) \prod_{n_r=1}^{N_r} \prod_{k, n_r \in V(n)} I_{f_k^{n_r} \rightarrow v_n^m}^l(b_n^m), \quad (16)$$

$$q_{k, n_r}^t(b_n^m) \propto \sum_{\bar{b}_n^m \neq b_n^m} p(y_k^{n_r} | \bar{b}_n^m) \prod_{n, m \in F(k, n_r)} I_{v_n^m \rightarrow f_k^{n_r}}^t(b_n^m). \quad (17)$$

The above procedure can be understood as the messages propagation over the SCMA graph depicted in Fig. 2. It treats the messages exchanged between VNs and FNs as continuous random variables and approximates the true distribution with a Gaussian distribution, characterized by its mean and variance. This approach enables signal detection to be transformed into the computation of mean and variance, avoiding the need to traverse all symbols. Specifically, we have

$$\text{Proj}_{\Phi}(q_0^t(b_n^m)) \propto \mathcal{CN}(\mu_{n, m}^t, \xi_{n, m}^t), \quad (18a)$$

$$I_{v_n^m \rightarrow f_k^{n_r}}^t(b_n^m) \propto \mathcal{CN}(\mu_{n, m \rightarrow k, n_r}^t, \xi_{m, t \rightarrow k, n_r}^t), \quad (18b)$$

$$I_{f_k^{n_r} \rightarrow v_n^m}^t(b_n^m) \propto \mathcal{CN}(\mu_{k, n_r \rightarrow n, m}^t, \xi_{k, n_r \rightarrow n, m}^t). \quad (18c)$$

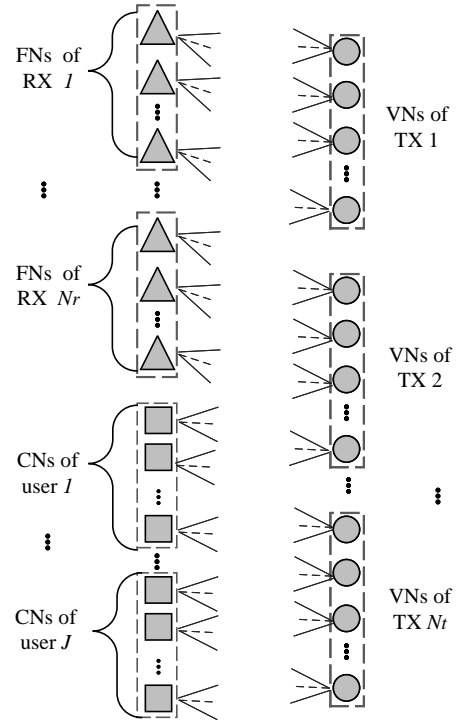


Fig. 2: An example of the proposed SSG.

In the following, we present the detailed message propagation in the proposed SSG. Denote c_l^j as the l th LDPC check node (CN) of user j . For simplicity, the superscript j is omitted.

1) *Initialization*: Assuming there is no *a priori* probability available, initial LLRs are set to zeros. Namely,

$$L_{v_n^m \rightarrow c_i} = 0, \quad L_{c_i \rightarrow v_n^m} = 0, \quad \forall i, \forall n, \forall m, \quad (19)$$

where $L_{v_n^m \rightarrow c_i}$ and $L_{c_i \rightarrow v_n^m}$ denote the LLRs propagating from the VN v_n^m to the i th LDPC CN and the opposite direction, respectively.

2) *Update of VNs to CNs and FNs*: The updating of VNs to CNs can be calculated as

$$L_{v_n^m \rightarrow c_i} = \sum_{(k, n_r) \in V(n)} L_{f_k^{n_r} \rightarrow v_n^m} + \sum_{i' \in \eta(n, m) \setminus i} L_{c_{i'} \rightarrow v_n^m}, \quad (20)$$

where $\eta(n, m)$ denotes the set of CNs connected to VN v_n^m and $L_{f_k^{n_r} \rightarrow v_n^m}$ denotes the LLR propagated from the FN $f_k^{n_r}$ to the VN v_n^m .

To update the message from VNs to FNs, each VN first gathers the LLR from both CNs and FNs, i.e.,

$$L(v_n^m) = \sum_{(k, n_r) \in V(n) \setminus (k, n_r)} L_{f_k^{n_r} \rightarrow v_n^m} + \sum_{i \in \eta(n, m)} L_{c_i \rightarrow v_n^m}. \quad (21)$$

Upon obtaining $L(v_n^m)$, the mean and variance of the VN v_n^m can be calculated as [15]

$$\begin{aligned}\mu_{n,m}^t &= 1 - 2p(b_{n,m} = -1|\mathbf{y}) \\ &= \frac{1 - \exp(L(v_n^m))}{1 + \exp(L(v_n^m))}, \\ \xi_{n,m}^t &= \sum_{u_{n,m} \in \{-1,1\}} p(b_{n,m} = u_{n,m} | \mathbf{y}) |u_{n,m} - \mu_{n,m}^t|^2.\end{aligned}\quad (22)$$

To proceed, denoted $\mu_{n,m \rightarrow k, n_r}^t$ and $\xi_{n,m \rightarrow k, n_r}^t$ by the mean and variance passing from VN v_n^m to FN $f_k^{n_r}$ at t th iteration, respectively. Based on the EP principles, one has the $\mu_{n,m \rightarrow k, n_r}^t$ and $\xi_{n,m \rightarrow k, n_r}^t$ updated as follows:

$$\begin{aligned}\xi_{n,m \rightarrow k, n_r}^t &= \left(\frac{1}{\xi_{n,m}^t} - \frac{1}{\xi_{k, n_r \rightarrow n, m}^{t-1}} \right)^{-1}, \\ \mu_{n,m \rightarrow k, n_r}^t &= \xi_{n,m \rightarrow k, n_r}^t \left(\frac{\mu_{n,m}^t}{\xi_{n,m}^t} - \frac{\mu_{k, n_r \rightarrow n, m}^{t-1}}{\xi_{k, n_r \rightarrow n, m}^{t-1}} \right),\end{aligned}\quad (23)$$

where $\mu_{k, n_r \rightarrow n, m}^t$ and $\xi_{k, n_r \rightarrow n, m}^t$ denote the mean and variance passing from FN $f_k^{n_r}$ to VN v_n^m at t th iteration, respectively.

3) *Update of CNs and FNs to VNs:* Based on (17) and (18a)-(18c), the message in the opposite direction becomes

$$\mu_{k, n_r \rightarrow n, m}^t = \frac{y_k^{n_r} - Z_{k, n_r \rightarrow n, m}^t}{h_{k, n_r}^{n, m}}, \quad \xi_{k, n_r \rightarrow n, m}^t = \frac{N_0 + B_{k, n_r \rightarrow n, m}^t}{|h_{k, n_r}^{n, m}|^2}, \quad (24)$$

where

$$\begin{aligned}Z_{k, n_r \rightarrow n, m}^t &= \sum_{\substack{i, j \in F(k, n_r), \\ i \neq n, j \neq m}} h_{k, n_r}^{i, j} \mu_{i, j \rightarrow k, n_r}^{t-1}, \\ B_{k, n_r \rightarrow n, m}^t &= \sum_{\substack{i, j \in F(k, n_r), \\ i \neq n, j \neq m}} |h_{k, n_r}^{i, j}|^2 \xi_{i, j \rightarrow k, n_r}^{t-1}.\end{aligned}\quad (25)$$

Finally, the posterior probability of transmitted symbol in LLR domain is updated by

$$L_{f_r \rightarrow v_n^m}^t = \log \frac{1 - \mu_{n, r \rightarrow m, t}^t}{1 + \mu_{n, r \rightarrow m, t}^t}. \quad (26)$$

The LLR of the parity CN c_i is updated as

$$L_{c_i \rightarrow v_n^m} = \gamma^{-1} \left(\sum_{(n', m') \in \phi_i \setminus (n, m)} \gamma(L_{v_{n'}^{m'} \rightarrow c_i}) \right), \quad (27)$$

where $\phi_i \setminus (n, m)$ is the set of VNs (excluding v_n^m) that connect to the CN c_i , and $\gamma(x)$ and $\gamma^{-1}(x)$ are respectively defined as

$$\begin{aligned}\gamma(x) &= \text{sign}(x) \times \left(-\log \tan \frac{|x|}{2} \right), \\ \gamma^{-1}(x) &= (-1)^{\text{sign}(x)} \times \left(-\log \tan \frac{|x|}{2} \right),\end{aligned}\quad (28)$$

where $\text{sign}(x)$ denotes the the sign of x .

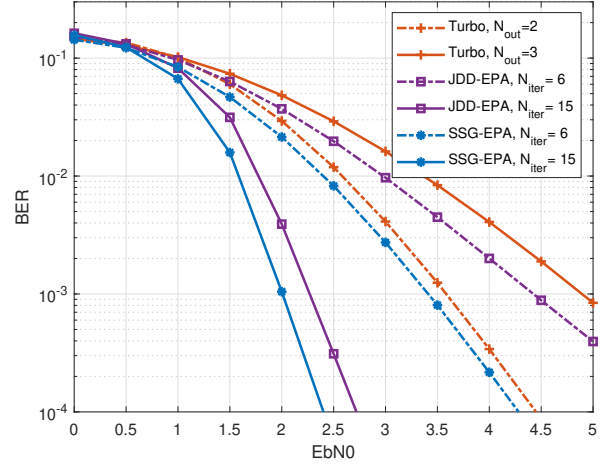


Fig. 3: BER comparison of different schemes for $N_t = 1$ and $N_r = 2$.

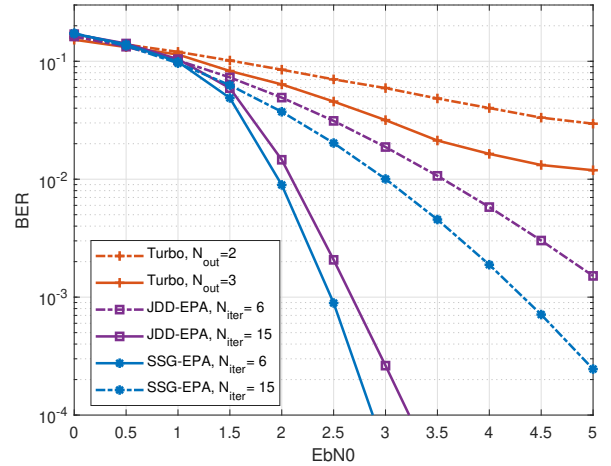


Fig. 4: BER comparison of different schemes for $N_t = 2$ and $N_r = 2$.

D. Computational Complexity

The computational complexity of EPA in the proposed SSG at each iteration can be approximated by $\mathcal{O}(N_{\text{SCMA}} N_r N_d f \log_2 M)$, where N_{SCMA} denotes the number of SCMA symbols at each LDPC block. Denoted d_c^{ldpc} where d_v^{ldpc} by the average column weight and the average row weight of the parity check matrix, respectively. Consequently, the complexity of LDPC decoding is $\mathcal{O}(2d_v^{\text{ldpc}} L_c + (J(2d_v^{\text{ldpc}} + 1)(L_c - L_b)))$, where L_c and L_b denote the number of coded bits and information bits, respectively [15]. The total complexities of the Turbo like IDD receiver and the proposed SSG-EPA are $N_{\text{iter}}^{\text{out}} (N_{\text{iter}}^{\text{EPA}} \mathcal{O}(\text{EPA}) + N_{\text{iter}}^{\text{LDPC}} \mathcal{O}(\text{LDPC}))$ and $N_{\text{iter}} (\mathcal{O}(\text{EPA}) + \mathcal{O}(\text{LDPC}))$, respectively.

IV. SIMULATION RESULTS

This section compares the error rate performance of the proposed SSG-EPA with the bench-marking schemes. Specifically, we consider an uplink SCMA system where the BS equipped $N_r = 2$ receive antennas and servers $J = 6$ users over $K = 4$ orthogonal resources. The codebook size is $M = 4$ and the signal space diversity codebook in [16] is used. The LDPC code with the number of information bits and the coded bits given by 200 and 400, respectively, and rate of 1/2 is used. Therefore, each LDPC frame consists of N_{SCMA} SCMA symbols for each user. The maximum number of iterations of the JSG-EPA and JDD-EPA receiver is $N_{iter} = 15$. For the turbo like IDD-EPA receiver, the outer loop iterations are $N_{iter}^{out} = 3$, and the number of inner loop iterations for both EPA and LDPC is given by $N_{iter}^{LDPC} = N_{iter}^{EPA} = 5$.

Fig. 3 shows the coded BER performances of the proposed SSG-EPA, the JDD-EPA and the IDD-EPA receivers with each user equipped a single antenna. As can be seen from the figure, the proposed SSG-EPA achieves the best BER performance among the bench-marking schemes. Specifically, the proposed SSG-EPA achieves about 0.2 dB and 1.5 dB than that of the JDD-EPA and the IDD-EPA receivers for $N_{iter} = 15$, respectively. Fig. 4 shows the BER comparison of different schemes for $N_t = 2$. It should be noted that the same codebook is applied to two transmit antennas. Again, the proposed SSG-EPA still achieves the best BER performance. Both SSG-EPA and JDD-EPA outperform the IDD-EPA receiver significantly. As the two transmit antennas are employed for multiplexing, the equivalent system is an overloaded system, i.e., $JN_t > KN_r$. In this case, the performance of the EPA with inner iterations degrades significantly, leading to a performance deterioration of the IDD-EPA receiver. Moreover, the JSG-EPA and JDD-EPA for $N_t = 2$ show about 0.5 dB performance degradation at $BER = 10^{-4}$ of $N_{iter} = 15$ compared to that of $N_t = 1$ in Fig. 3.

Fig. 5 shows the coded BER performance for different number of iterations of the proposed SSG-EPA and JDD-EPA for $N_t = 1$ and $N_r = 2$. As can be seen from the figure, JDD-EPA and SSG-EPA need about 20 and 16 iterations for convergence at the $E_b/N_0 = 2.5$ dB, respectively.

V. CONCLUSION

In this paper, we proposed a SSG-EPA for uplink MIMO-SCMA. By reformulating the codebook with a linear encoding model, the VNs of SCMA can be transformed from symbol-level to bit-level VNs. Leveraging this transformation, a SSG has been proposed by emerging the sparse graphs of SCMA and LDPC into an integrated one. In addition, we have investigated the use of EPA in the SSG for low-complexity detection, resulting in the SSG-EPA receiver. Notably, the proposed SSG-EPA can update the belief message in a one-shot manner. Namely, both SCMA and LDPC graphs are updated simultaneously, eliminating the use of interleavers, de-interleavers, symbol-to-bit, and bit-to-symbol LLR transformations. Simulation results showed that the proposed SSG-EPA

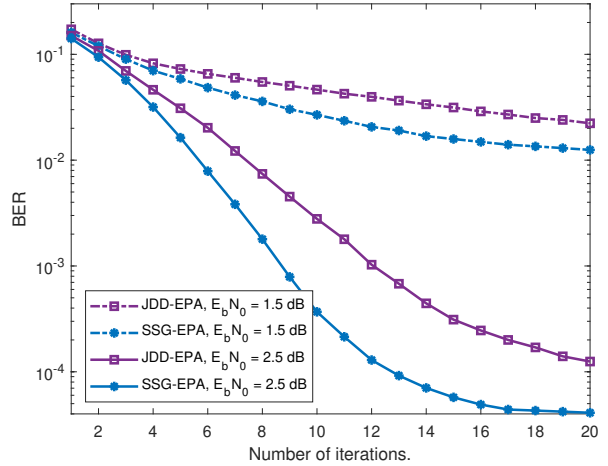


Fig. 5: BER performance v.s. number of iterations.

achieves better error rate performance than the state-of-the-art schemes.

REFERENCES

- [1] L. Yu, Z. Liu, M. Wen, D. Cai, S. Dang, Y. Wang, and P. Xiao, "Sparse code multiple access for 6G wireless communication networks: Recent advances and future directions," *IEEE Commun. Stand. Mag.*, vol. 5, no. 2, pp. 92–99, 2021.
- [2] Q. Luo, Z. Mheich, G. Chen, P. Xiao, and Z. Liu, "Reinforcement learning aided link adaptation for downlink NOMA systems with channel imperfections," in *2023 IEEE WCNC*, 2023, pp. 1–6.
- [3] Z. Ding and H. V. Poor, "Joint beam management and power allocation in THz NOMA networks," *IEEE Trans. Commun.*, vol. 71, no. 4, pp. 2059–2073, 2023.
- [4] H. Wen, Z. Liu, Q. Luo, C. Shi, and P. Xiao, "Designing enhanced multidimensional constellations for code-domain NOMA," *IEEE Wireless Commun. Lett.*, vol. 11, no. 10, pp. 2130–2134, 2022.
- [5] Q. Luo, P. Gao, Z. Liu, L. Xiao, Z. Mheich, P. Xiao, and A. Maaref, "An error rate comparison of power domain non-orthogonal multiple access and sparse code multiple access," *IEEE Open J. Commun. Society*, vol. 2, pp. 500–511, 2021.
- [6] H. Cheng, C. Zhang, Y. Huang, and L. Yang, "Efficient message passing receivers for downlink MIMO-SCMA systems," *IEEE Trans. Veh. Technol.*, vol. 71, no. 5, pp. 5073–5086, 2022.
- [7] X. Meng, Y. Wu, Y. Chen, and M. Cheng, "Low complexity receiver for uplink SCMA system via expectation propagation," in *2017 IEEE WCNC*, 2017, pp. 1–5.
- [8] P. Wang, L. Liu, S. Zhou, G. Peng, S. Yin, and S. Wei, "Near-optimal MIMO-SCMA uplink detection with low-complexity expectation propagation," *IEEE Trans. Wireless Commun.*, vol. 19, no. 2, pp. 1025–1037, 2020.
- [9] A. Bayesteh, H. Nikopour, M. Taherzadeh, H. Baligh, and J. Ma, "Low complexity techniques for SCMA detection," in *IEEE GC Wkshps*, 2015, pp. 1–6.
- [10] J. Xiao, J. Hu, and K. Han, "Low complexity expectation propagation detection for SCMA using approximate computing," in *2019 IEEE GLOBECOM*, 2019, pp. 1–6.
- [11] Z. Zhang, H. Li, Y. Dong, X. Wang, and X. Dai, "Decentralized signal detection via expectation propagation algorithm for uplink massive MIMO systems," *IEEE Trans. Veh. Technol.*, vol. 69, no. 10, pp. 11 233–11 240, 2020.
- [12] J. Bao, Z. Ma, M. Xiao, T. A. Tsiftsis, and Z. Zhu, "Bit-interleaved coded SCMA with iterative multiuser detection: Multidimensional constellations design," *IEEE Trans. Commun.*, vol. 66, no. 11, pp. 5292–5304, 2018.
- [13] B. Ren, S. Han, W. Meng, C. Li, X. Wu, and X. Sha, "Enhanced turbo detection for SCMA based on information reliability," in *2015 IEEE ICC*, 2015, pp. 1–5.

- [14] Z. Zhang, K. Han, J. Hu, and J. Chen, "Joint detection and decoding schemes for turbo coded SCMA systems," in *2016 IEEE GC Wkshps*, 2016, pp. 1–6.
- [15] L. Chai, Z. Liu, P. Xiao, A. Maaref, and L. Bai, "An improved epa-based receiver design for uplink LDPC coded SCMA system," *IEEE Wireless Commun. Lett.*, vol. 11, no. 5, pp. 947–951, 2022.
- [16] Q. Luo, Z. Liu, G. Chen, and P. Xiao, "Enhancing signal space diversity for SCMA over Rayleigh fading channels," *IEEE Trans. Wireless Commun.*, vol. 23, no. 4, pp. 3676–3690, 2024.
- [17] Q. Luo, Z. Liu, G. Chen, Y. Ma, and P. Xiao, "A novel multitask learning empowered codebook design for downlink SCMA networks," *IEEE Wireless Commun. Lett.*, vol. 11, no. 6, pp. 1268–1272, 2022.